Effect of Spatial Inhomogeneity in Dielectric Permittivity on DNA Double Layer Formation

J. R. C. van der Maarel
Department of Biochemistry, University of Minnesota, St. Paul, Minnesota 55108 USA

ABSTRACT In solutions of tetramethylammonium (TMA^+) DNA (double stranded) without added low-molecular-weight salt, the counterion radial density is calculated using the cylindrical Poisson-Boltzmann equation with a distance-dependent quasimacroscopic dielectric permittivity. Comparisons with small-angle neutron scattering data indicate that any inhomogeneity in dielectric permittivity is confined to one or two solvent layers from the DNA surface. At least for TMA^+, which may be too large to penetrate the grooves of DNA to any significant extent, dielectric inhomogeneity modeled in this way has no detectable effect on the radial distribution.

INTRODUCTION

Many properties of DNA are governed by electrostatic interactions between the negatively charged phosphate moieties, positively charged counterions, and simple salt. Because of strong Coulomb interactions, small ions accumulate about DNA and a double layer is formed. The formation of the double layer has important consequences for, e.g., thermodynamic properties and inter- and intramolecular organization (Katchalsky, 1971; Onsager, 1949; Anderson and Record, 1995). An example of the latter category is the electrostatic free energy difference between different double-helical DNA configurations (e.g., B- and Z-form; Lukashin et al., 1991a). Most models in theoretical studies and interpretations of experimental data treat the small ions as charged spheres and DNA as charged wormlike polymers embedded in a uniform medium with a dielectric constant of ~80. According to some theoretical and experimental assessments, the dielectric constant inside the grooves and near the surface takes much lower values (Jayaram et al., 1989; Mazur and Jernigan, 1991). In particular, Jin and Breslauer (1988) reported a dielectric constant of ~20 within the minor groove of the poly[d(AT)]·poly[d(AT)] duplex from the fluorescence properties of a minor groove-directed binding ligand. A low local dielectric constant might be related to the presence of a dielectric boundary, changes in the water structure, and the presence of high ion concentrations. The range of the inhomogeneity in dielectric permittivity is unknown, but theoretical studies show that the bulk value is recovered within a few angstroms of the DNA surface (Lamm and Pack, 1997; Jayaram and Beveridge, 1996). It is conjectured, however, that the variation in the dielectric constant has a significant effect on the local counterion distribution and electrostatic free energy (Jayaram et al., 1990; Lukashin et al., 1991b).

The structural arrangement of counterions near DNA can be inferred from neutron or x-ray scattering methods, if the momentum transfer is on the order of the inverse double layer thickness. The scattered intensities are sensitive to the set of spatial Fourier transforms of the DNA, DNA-counterion, and counterion density correlation functions (partial structure functions; Lovesey, 1984). Small-angle neutron scattering (SANS) methods based on the variation in isotopic composition of either solvent or solute have made it possible to determine individual partial structure functions in solutions of mononucleosomal DNA fragments and polystyrenesulfonate (PSS) coils with tetramethylammonium (TMA^+) counterions (van der Maarel et al., 1992a, 1993; Groot et al., 1994; Kassapidou et al., 1997, 1998a). It was seen that by optimizing some of the geometric parameters, the classical or modified Poisson-Boltzmann (PB) equation with uniform permittivity gives a good description of the structure (Alfrey et al., 1951; Fuoss et al., 1951; Bhuiyan et al., 1996). Chang et al. (1990, 1991) investigated the distribution of heavy metal Cs^+ and Tl^+ about DNA and cylindrical micelles with small-angle x-ray scattering (SAXS). The intensities compared favorably with the relevant combination of partial structure functions derived from the PB equation, provided a considerable fraction of Cs^+ and Tl^+ counterions penetrate the DNA grooves. This effect was not observed in the TMA-DNA SANS investigations, probably because of a difference in cation radius between the relatively bulky TMA^+ cation and the heavy metal ions.

I thought it of interest to gauge the effect of inhomogeneity in dielectric permittivity by a comparison of previously reported SANS data with the prediction of PB theory, including a quasimacroscopic radial dependence of the dielectric constant (Lukashin et al., 1991b). The PB calculations are made using several representations of the dielectric response, ranging from uniform through a series of functions by which the dielectric constant varies from a low value at the DNA surface to the bulk value at various distances from the surface. The radial counterion density

Received for publication 9 July 1998 and in final form 4 January 1999.

Address reprint requests to Dr. Johan R. C. van der Maarel, Gorlaeus Laboratories, Leiden University, P.O. Box 9502, 2300 RA Leiden, The Netherlands. Tel.: 31-71-5274543; Fax: 31-71-5274397; E-mail: j.maarel@rulgca.leidenuniv.nl.

Dr. van der Maarel is on leave from Leiden University.

0006-3495/99/05/2673/06 $2.00

profile is inferred from previously published SANS experiments on 163-bp DNA fragments. Electrostatic interactions are most important under minimal screening conditions, and, hence, the ionic strength was kept as low as possible without the addition of simple electrolyte. A limitation of the present approach is that TMA^+ counterions (which are necessary for sufficient neutron scattering contrast) cannot penetrate the grooves and/or come very near to the surface. Accordingly, we can only probe the medium dielectric response beyond a certain distance from the DNA spine axis, determined by the physical extent of the DNA molecule, intermediate hydration water, and counterion size.

THEORY

For polyelectrolytes without added simple salt, a self-consistent solution charge distribution can be obtained from the solution of the PB equation and the cell model (Alfrey et al., 1951; Fuoss et al., 1951). The requirement for applying the cell model is that the DNA chain is locally rodlike over a length far exceeding the double layer thickness and bearing a sufficiently large number of charges. Theory and computer simulation show that the effect of the discreteness of the DNA charges on the counterion concentration profile is generally small and dwindles a few angstroms from the DNA surface (Conrad et al., 1988; Hochberg et al., 1994). The fragment is assumed to be a uniformly charged rod with length L and is placed along the z axis of a coaxial cylinder of the same length L and radius r_{cell}. The cell radius is determined by the nucleotide concentration ρ by $\rho A\pi r_{cell}^2 = 1$, with the longitudinal axis projected nucleotide repeat distance $A = 0.171$ nm. Electroneutrality requires compensation of the total DNA charge by the mobile simple counterion charges within the cell volume. In the longitudinal direction, along the DNA axis, the nucleotide monomer (m) and counterion (c) distributions are assumed to be uniform. Away from this axis, the corresponding densities are given by the radial profiles $\rho_m(r)$ and $\rho_c(r)$, respectively.

Structure functions

The charge distribution and radial density profiles (obtained from the PB equation) can be assessed by comparison with experimental scattering data. The scattered intensities are sensitive to the partial structure functions, which are the spatial Fourier transforms of the DNA, DNA-counterion, and counterion density correlation functions. For correlations within a single cell volume, the partial structure functions have been evaluated by van der Maarel et al. (1992a). However, for lower values of momentum transfer and/or higher DNA density, correlations between different cell volumes become progressively more important, and the experimental data deviate from the single-cell calculations. In the case of neutron radiation the condition $qL \gg 1$ is often fulfilled, and one essentially probes local structure about the polyion. Furthermore, the high DNA linear charge density confines most counterions to the immediate vicinity of the macroion, and the concentration at the cell boundary is much lower than the average value. If fluctuations in radial densities are neglected (at the same level of approximation as the PB equation), the partial structure functions can be expressed, to a good approximation, as a product of terms involving the radial profiles and a term related to the polymer structure with vanishing cross section (Kassapidou et al., 1997, 1998a). Taking the ratio of the nucleotide-counterion S_{mc} and nucleotide monomer S_{mm} structure function eliminates the polymer structure:

$$\frac{S_{mc}(q)}{S_{mm}(q)} = \frac{a_c(q)}{a_m(q)}, \quad qL \gg 1 \tag{1}$$

with the cylindrical Fourier (Hankel) transformation

$$a_i(q) = 2\pi \int_0^{r_{cell}} dr\, r\, J_0(qr)\rho_i(r) \quad (i = m, c) \tag{2}$$

and J_0 denotes the zero-order Bessel function of the first kind. From the full set of partial structure functions, information on the radial counterion density profile can be obtained without resorting to a model of (inter- and intra-) chain correlations (Kassapidou et al., 1997, 1998a). In the long wavelength limit ($q \to 0$) electroneutrality requires that the ratio in Eq. 1 goes to unity.

Radial profiles

Transform (Eq. 2) can be further evaluated using analytical expressions of the radial densities. If the radial DNA density is assumed to be uniform for $0 \le r \le r_p$ and is given by $\rho_m(r)\pi r_p^2$ and zero for $r > r_p$, where r_p is the DNA radius, one obtains

$$a_m(q) = \frac{2J_1(qr_p)}{qr_p} \tag{3}$$

where J_1 is the first-order Bessel function of the first kind. The DNA cross section might also be described by a Gaussian radial density profile with second moment, $\langle r^2 \rangle = r_p^2/2$. In the present range of momentum transfer, the Hankel transform of such a Gaussian profile is very similar to Eq. 3, and the radius r_p can be interpreted as a cross-sectional radius of gyration.

The radial counterion density profile can be obtained from the solution of the PB equation. Apart from the cell radius, the other structural parameters are the distance of closest approach between the counterion center of mass and the DNA spine axis r_c and the linear charge density $\xi = Q/A$, where Q is the Bjerrum length ($Q = e^2/4\pi\epsilon_B kT$). The distance of closest approach is not necessarily equal to the DNA radius r_p; rather, one expects a slightly larger value due to counterion size and intermediate hydration water. Without added simple salt, the dimensionless potential sat-

isfies the PB equation

$$[r\epsilon(r)\phi'(r)]' = -4\pi Q\epsilon_B\rho_R\exp[-\phi(r)] \quad (4)$$

with boundary conditions

$$\phi'(r_c) = \frac{2\xi}{r_c}\frac{\epsilon_B}{\epsilon(r_c)}, \quad \phi(r_{cell}) = 0 \quad (5)$$

Here the prime denotes differentiation with respect to the radial coordinate r, ρ_R is the counterion concentration at the cell boundary, and ϵ_B is the bulk dielectric constant of the solvent. Equation 4 allows for a quasimacroscopic inhomogeneity of the medium through a spatially dependent dielectric constant $\epsilon(r)$. The permittivity should change continuously from the value ϵ_P at the DNA surface (at radial distance r_O) to the bulk value at larger distances. The radial dependence is unknown, but I will adopt the approximation of Lukashin et al. (1991b):

$$\frac{1}{\epsilon(r)} = \frac{1}{\epsilon_P} + \left[\frac{1}{\epsilon_P} - \frac{1}{\epsilon_B}\right]\frac{r - r_o}{\lambda_\epsilon}K_1\left(\frac{r - r_o}{\lambda_\epsilon}\right) \quad (6)$$

where K_1 is the first-order modified Bessel function and λ_ϵ denotes the correlation length. In the standard model, $\epsilon(r)$ is constant at any distance ($\epsilon(r) = \epsilon_B$, i.e., $\lambda_\epsilon = 0$), and the PB equation can be solved analytically (Alfrey et al., 1951; Fuoss et al., 1951). In the case of a spatially dependent dielectric constant, the radial counterion profile and its Hankel transform (Eq. 2) have to be evaluated by numerical procedures.

RESULTS AND DISCUSSION

The partial structure functions for 163-bp DNA fragments were measured by SANS and contrast matching in water (Groot et al., 1994). The counterion was TMA^+, and there was no added low-molecular-weight salt in solution. Fig. 1 displays the ratio of the nucleotide-counterion and the nucleotide (DNA) structure function for 0.05 mol nucleotides/dm^3. More data on 1100-bp DNA and 0.1 mol nucleotides/dm^3 163-bp DNA are available (van der Maarel et al., 1992a; Kassapidou et al., 1997, 1998a), but they show the same features and are not presented here.

The fragments can be considered as semiflexible rodlike molecules, because the contour length (55 nm) is approximately equal to the DNA persistence length (50 nm). Within the present experimental range of momentum transfer ($qL > 10$), the scattering data are sensitive to correlations over distances on the order of the double layer thickness, and effects of finite contour length and/or flexibility are negligible. The intrachain structure can be described, to a good approximation, by the high q limiting form of the form function of a rod with a finite cross section. In previous work, the second moment of the cross section (i.e., radius of gyration) and the nucleotide repeat distance were obtained from a fit in the presence of excess salt to suppress intermolecular interference (van der Maarel and Kassapidou, 1998). These parameters take the values 0.8 and 0.17 nm, respectively, in close agreement with the expected values for a double helix in the B-form. The distance of closest approach between the counterion center of mass and the DNA spine axis was obtained from a fit of the classical PB results (with uniform medium permittivity) to the experimental partial structure functions and takes the value r_c = 1.4 nm (van der Maarel et al., 1992a). The relevant structural parameters are collected in Table 1.

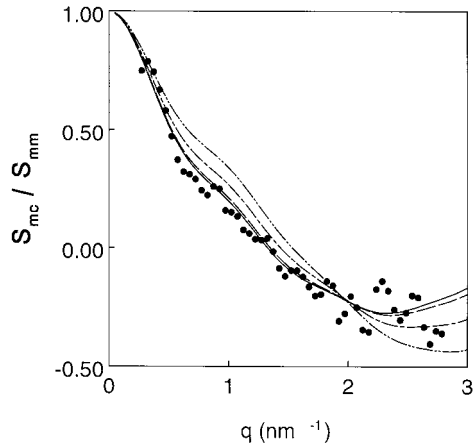

FIGURE 1 Nucleotide-counterion partial structure function divided by the nucleotide (DNA) partial structure function versus momentum transfer. The nucleotide concentration amounts to 0.05 mol/dm^3. The lines represent the ratio in Eq. 1, calculated with the structural parameters in Table 1, and radial counterion profiles calculated with dielectric correlation lengths λ_ϵ (in nm): 0 (——); 0.1 (– – –); 0.15 (– · –); 0.2 (– ·· –).

The derived cross-sectional radius of gyration (0.8 nm) is slightly smaller than the DNA outer radius of 1 nm, which is due to the relatively open molecular structure and the existence of grooves. The relatively large value of r_c can be rationalized in terms of the physical extent of the DNA molecule, hydration water, and counterion size. In TMACl solutions with cation concentrations similar to those within the DNA double layer, intermolecular correlations about TMA^+ start rising at ~0.36 nm and peak at ~0.46 nm from the nitrogen atom (Finney and Turner, 1988). The first hydration shell comprises 20 ± 2 water molecules, irrespective of concentration in the range 0.5–1.9 mol/kg. Accordingly, if the TMA^+ counterions are drawn into close contact with the DNA phosphates with a concurrent displacement of hydration water, r_c is expected to take a value around 1.4 nm. The relatively large intermolecular correlation distance and the extended hydration structure of the TMA^+ ion

TABLE 1 Various geometric parameters for 163-bp DNA (in nm)

A	r_p	r_o	r_c	r_{cell}	L_p	L
0.171	0.8	1.0	1.4	7.9	50	57

A, Spine axis projected repeat distance; r_p, DNA radius; r_o, outer radius; r_c, distance of closest approach; r_{cell}, cell radius (0.05 mol nucleotides/L); L_p, persistence length; L, contour length.

prevent significant penetration of the grooves and/or very close approach to the DNA surface. A less effective DNA charge screening by TMA^+ counterions is also indicated by a 5° downward shift of the duplex melting temperature (irrespective of ionic strength) and a slight upward shift of the critical phase boundary concentrations pertaining to liquid crystal formation (Kassapidou et al., 1998b and unpublished results).

The data displayed in Fig. 1 can be interpreted with Eqs. 1 and 2, together with radial density profiles for nucleotides and counterions away from the DNA spine axis. To gauge the effect of a spatially dependent dielectric permittivity, the counterion profile and its Hankel transform $a_c(q)$ were calculated for four different values of the dielectric correlation length $\lambda_\epsilon = 0$ (i.e., $\epsilon(r) = \epsilon_B$), 0.1, 0.15, and 0.2 nm, respectively. The spatially dependent dielectric response (Eq. 6) is displayed in Fig. 2. At the DNA outer radius, $r_O = 1$ nm, the dielectric constant was set at a value of 4.0, and the bulk constant was fixed at $\epsilon_B = 78.4$. The PB equation was numerically solved with fourth- and fifth-order Runge-Kutta formulas, and the counterion concentration at the cell boundary ρ_R was optimized to satisfy boundary conditions (Eq. 5) (Matlab numeric computation software; The Math Works, Natick, MA). In the calculation of the potential, the distance of closest approach, cell radius, and nucleotide (charge) repeat distance were fixed at their nominal values (Table 1). Fig. 3 displays the calculated radial counterion concentration profiles. Hankel transforms of the counterion profiles divided by the nucleotide profile are shown in Fig. 1. The calculated ratio (Eq. 1) goes correctly to unity in the $q \rightarrow 0$ limit, which confirms the convergence of the numerical procedures.

With increasing dielectric correlation length, the counterion concentration close to the DNA surface increases with a concurrent decrease at the cell boundary. Stronger confinement translates into a scaling of the transform $a_c(q)$ and, hence, of the ratio in Eq. 1 toward higher values of momentum transfer. As can be seen in Fig. 1, the best agreement is observed when the correlation length λ_ϵ does not exceed 0.1 nm. In the present range of momentum transfer, variation of the DNA cross section within reasonable limits has little influence on the general features.

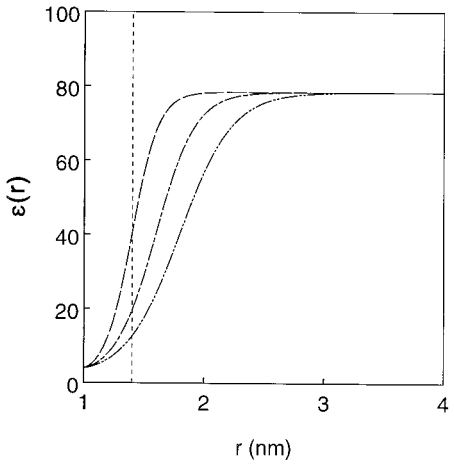

FIGURE 2 Medium dielectric response versus radial distance away from the DNA spine axis. The curves are calculated according to Eq. 6 with correlation lengths λ_ϵ (in nm): 0.1 (– – –); 0.15 (– · –); 0.2 (– ·· –). The value of ϵ_P was set at 4.0, and the bulk constant ϵ_B was fixed at the value 78.4. The dashed vertical denotes the distance of closest approach, $r_c = 1.4$ nm.

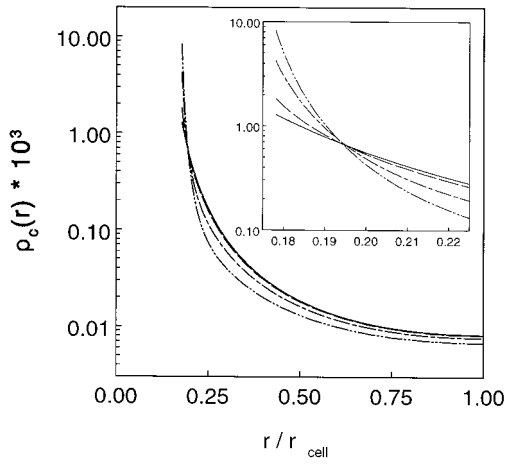

FIGURE 3 Counterion concentration profile versus distance away from the DNA axis. The curves are calculated according to Eqs. 4–6 with the structural parameters in Table 1 and correlation lengths λ_ϵ (in nm): 0 (——); 0.1 (– – –); 0.15 (– · –); 0.20 (– ·· –). The inset displays the inner double-layer region.

In addition to the dielectric correlation length, the counterion profile depends on the assigned values of the distance of closest approach, cell radius, and DNA charge repeat distance. The cell radius is fixed through concentration, and the nucleotide repeat distance is well known. Of particular importance is the distance of closest approach; its value was obtained from an optimization of the PB results with a uniform medium dielectric constant to the experimental SANS data (van der Maarel et al., 1992a). The decay length of the inner double layer is inversely proportional to surface charge density (Rouzina and Bloomfield, 1996), and, hence, to a very good approximation the transform $a_c(q)$ scales with the inverse of the distance of closest approach. A second effect of a smaller r_c value is similar to an increase in dielectric correlation length, because closer to the DNA surface counterions experience a lower dielectric permittivity (see Fig. 2). Accordingly, a smaller distance of closest approach cannot compensate for the effect of a larger correlation length, because a decrease in r_c and an increase in λ_ϵ have a similar effect on the structure functions. A larger r_c value is unlikely in view of the physical extent of the DNA molecule and TMA^+ counterion.

The partial structure functions are calculated, neglecting small ion correlations and density fluctuations. These effects potentially modify the scattering for two reasons: 1) they result in a change of the average counterion profile and 2) they give an additional scattering contribution (van der Maarel et al., 1992b; Auvray and de Gennes, 1986). For

highly charged polyelectrolytes, the additional scattering contribution has not been evaluated yet, but it does not affect the ratio in Eq. 1 (because of the heterodyne interference between amplitudes scattered by the DNA and counterions) and it is expected to be modest in comparison with the pronounced contribution due to the average profile. In the case of monovalent counterions without added simple salt, theoretical calculation in the modified PB approach shows that the change in average profile is almost negligible and has no significant effect on the structure functions (Bhuiyan et al., 1996). Furthermore, theoretical work and computer simulation show that ionic correlation and fluctuation effects generally result in an increase in counterion density close to the DNA surface (see, e.g., Das et al., 1995) and, again, cannot compensate for the effect of a larger dielectric correlation length.

CONCLUSIONS

The DNA molecule is suitable for a critical test of the radial counterion profile, because it is relatively highly charged and its molecular dimensions are fairly well known. The size of the TMA^+ counterions and its hydration structure prevent significant penetration of the grooves, which is manifested by the value of $r_c = 1.4$ nm. The scattering data are sensitive to the counterion concentration profile and, hence, a spatial inhomogeneity in dielectric constant. However, the data can be well described with the counterion distribution obtained from the PB equation with a dielectric correlation length less than, say, 0.1 nm. This figure should be interpreted as an upper bound, because any lowering of the dielectric constant at a shorter distance scale or inside the grooves escapes detection because TMA^+ counterions cannot come very close to the DNA surface. It should be noted that small ions remain hydrated when they accumulate around a highly charged polymer, and, except for penetration of the grooves, their spatial distribution is expected to be similar (van der Maarel et al., 1989; Bieze et al., 1994). Any stronger confinement or accumulation of counterions closer to DNA (caused by, e.g., hydrophobic interactions, ion correlation effects, etc.) results in a scaling of the ratio of the structure functions toward higher values of momentum transfer and cannot compensate for the effect of a larger dielectric correlation length. The range of the inhomogeneity in dielectric permittivity induced by the DNA surface is confined to one or two molecular solvent layers and is in agreement with previous theoretical and computer simulation work (Jayaram et al., 1990; Lamm and Pack, 1997; Jayaram and Beveridge, 1996). This conclusion does not rely on the particular function $\epsilon(r)$; other semiempirical expressions with similar dielectric correlation lengths would give similar results.

Ioulia Rouzina and Victor Bloomfield are gratefully acknowledged for many stimulating discussions and critical reading of the manuscript.

The Netherlands Organization for Scientific Research (NWO) is thanked for a travel grant.

REFERENCES

Alfrey, T., Jr., P. W. Berg, and H. Morawetz. 1951. The counterion distribution in solutions of rod-shaped polyelectrolytes. *J. Polym. Sci.* 7:543–547.

Anderson, C. F., and M. T. Record, Jr. 1995. Salt-nucleic acid interactions. *Annu. Rev. Phys. Chem.* 46:657–700.

Auvray, L., and P. G. de Gennes. 1986. Neutron scattering by adsorbed polymer layers. *Europhys. Lett.* 2:647–650.

Bhuiyan, L. B., C. W. Outhwaite, and J. R. C. van der Maarel. 1996. Structure functions of rodlike DNA fragment and polystyrenesulfonate solutions in the modified Poisson-Boltzmann theory. *Physica A.* 231: 295–303.

Bieze, T. W. N., R. H. Tromp, J. R. C. van der Maarel, M. H. J. M. van Strien, M.-C. Bellissent-Funel, G. W. Neilson, and J. C. Leyte. 1994. Hydration of chloride ions in a polyelectrolyte solution studied with neutron diffraction. *J. Phys. Chem.* 98:4454–4458.

Chang, S.-L., S.-H. Chen, R. L. Rill, and J. S. Lin. 1990. Measurements of monovalent and divalent counterion distributions around persistence length DNA fragments in solution. *J. Phys. Chem.* 94:8025–8028.

Chang, S.-L., S.-H. Chen, R. L. Rill, and J. S. Lin. 1991. Measurement and interpretation of counterion distribution around cylindrical polyelectrolytes. *Prog. Colloid Polym. Sci.* 84:409–415.

Conrad, J., M. Troll, and B. H. Zimm. 1988. Ions around DNA: Monte Carlo estimates of distribution with improved electrostatic potentials. *Biopolymers.* 27:1711–1732.

Das, T., D. Bratko, L. B. Bhuiyan, and C. W. Outhwaite. 1995. Modified Poisson-Boltzmann theory applied to linear polyelectrolyte solutions. *J. Phys. Chem.* 99:410–418.

Finney, J. L., and J. Turner. 1988. Direct measurement by neutron diffraction of the solvation of polar and apolar molecules. The hydration of the tetramethylammonium ion. *Faraday Discuss. Chem. Soc.* 85:125–135.

Fuoss, R. M., A. Katchalsky, and S. Lifson. 1951. The potential of an infinite rodlike molecule and the distribution of counter ions. *Proc. Natl. Acad. Sci. USA.* 37:579–589.

Groot, L. C. A., M. E. Kuil, J. C. Leyte, J. R. C. van der Maarel, J.-P. Cotton, and G. Jannink. 1994. Partial structure functions of DNA fragment solutions: concentration effects. *J. Phys. Chem.* 98:10167–10172.

Hochberg, D., T. W. Kephart, and G. Edwards. 1994. Structural information in the local electric field of dissolved B-DNA. *Phys. Rev. E.* 49:851–867.

Jayaram, B., and D. L. Beveridge. 1996. Modeling DNA in aqueous solutions: theoretical and computer simulation studies on the ion atmosphere of DNA. *Annu. Rev. Biophys. Biomol. Struct.* 25:367–394.

Jayaram, B., K. A. Sharp, and B. Honig. 1989. The electrostatic potential of B-DNA. *Biopolymers.* 28:975–993.

Jayaram, B., S. Swaminathan, D. L. Beveridge, K. Sharp, and B. Honig. 1990. Monte Carlo simulation studies on the structure of the counterion atmosphere of B-DNA. Variations on the primitive dielectric model. *Macromolecules.* 23:3156–3165.

Jin, R., and K. Breslauer. 1988. Characterization of the minor groove environment in a drug-DNA complex: bisbenzimide bound to the poly[d(AT)] · poly[d(AT)] duplex. *Proc. Natl. Acad. Sci. USA.* 85: 8939–8942.

Kassapidou, K., W. Jesse, M. E. Kuil, A. Lapp, S. Egelhaaf, and J. R. C. van der Maarel. 1997. Structure and charge distribution in DNA and poly(styrenesulfonate) (PSS) aqueous solutions. *Macromolecules.* 30: 2671–2684.

Kassapidou, K., W. Jesse, M. E. Kuil, A. Lapp, S. Egelhaaf, and J. R. C. van der Maarel. 1998a. Correction: structure and charge distribution in DNA and poly(styrenesulfonate) (PSS) aqueous solutions. *Macromolecules.* 31:1704.

Kassapidou, K., W. Jesse, J. A. P. P. van Dijk, and J. R. C. van der Maarel. 1998b. Liquid crystal formation in DNA fragment solutions. *Biopolymers.* 46:31–37.

Katchalsky, A. 1971. Polyelectrolytes. *Pure Appl. Chem.* 26:327–373.

Lamm, G., and G. R. Pack. 1997. Calculation of dielectric constants near polyelectrolytes in solution. *J. Phys. Chem. B.* 101:959–965.

Lovesey, S. W. 1984. Theory of Neutron Scattering from Condensed Matter, Vol. 1. Oxford University Press, Oxford.

Lukashin, A. V., D. B. Beglov, and M. D. Frank-Kamenetskii. 1991a. Comparison of different approaches for calculation of polyelectrolyte free energy. *J. Biol. Struct. Dyn.* 8:1113–1118.

Lukashin, A. V., D. B. Beglov, and M. D. Frank-Kamenetskii. 1991b. Allowance for spatial dispersion of dielectric permittivity in polyelectrolyte model of DNA. *J. Biol. Struct. Dyn.* 9:517–523.

Mazur, J., and R. L. Jernigan. 1991. Distance-dependent dielectric constants and their application to double-helical DNA. *Biopolymers.* 31: 1615–1629.

Onsager, L. 1949. The effect of shape on the interaction of colloidal particles. *Ann. N.Y. Acad. Sci.* 51:627–659.

Rouzina, I., and V. A. Bloomfield. 1996. Competitive electrostatic binding of charged ligands to polyelectrolytes: planar and cylindrical geometries. *J. Phys. Chem.* 100:4292–4304.

van der Maarel, J. R. C., L. C. A. Groot, J. G. Hollander, W. Jesse, M. E. Kuil, J. C. Leyte, L. H. Leyte-Zuiderweg, M. Mandel, J.-P. Cotton, G. Jannink, A. Lapp, and B. Farago. 1993. On the charge distribution in aqueous poly(styrenesulfonic acid) solutions: a small angle neutron scattering study. *Macromolecules.* 26:7295–7299.

van der Maarel, J. R. C., L. C. A. Groot, M. Mandel, W. Jesse, G. Jannink, and V. Rodriguez. 1992a. Partial and charge structure functions of monodisperse DNA fragments in salt free aqueous solution. *J. Phys. II France.* 2:109–122.

van der Maarel, J. R. C., and K. Kassapidou. 1998. Structure of short DNA fragment solutions. *Macromolecules.* 31:5734–5739.

van der Maarel, J. R. C., M. Mandel, and G. Jannink. 1992b. On the charge structure function of rodlike polyelectrolytes. *Europhys. Lett.* 20: 607–612.

van der Maarel, J. R. C., D. H. Powell, A. K. Jawahier, L. H. Leyte-Zuiderweg, G. W. Neilson, and M.-C. Bellissent-Funel. 1989. On the structure and dynamics of lithium counterions in polyelectrolyte solutions: a nuclear magnetic resonance and neutron scattering study. *J. Chem. Phys.* 90:6709–6715.